DESTRUCTION OF MOLECULAR GAS RESERVOIRS IN EARLY-TYPE GALAXIES BY ACTIVE GALACTIC NUCLEUS FEEDBACK

KEVIN SCHAWINSKI[1,2,3], CHRIS J. LINTOTT[1], DANIEL THOMAS[4], SUGATA KAVIRAJ[1], SERENA VITI[5], JOSEPH SILK[1],
CLAUDIA MARASTON[4], MARC SARZI[6], SUKYOUNG K. YI[7], SEOK-JOO JOO[7], EMANUELE DADDI[8], ESTELLE BAYET[3], TOM BELL[9],
AND JOE ZUNTZ[1]
[1] Department of Physics, University of Oxford, Oxford OX1 3RH, UK; kevin.schawinski@yale.edu
[2] Department of Physics, Yale University, New Haven, CT 06511, USA
[3] Yale Center for Astronomy and Astrophysics, Yale University, P.O. Box 208121, New Haven, CT 06520, USA
[4] Institute of Cosmology & Gravitation, University of Portsmouth, Portsmouth, PO1 2EG, UK
[5] Department of Physics and Astronomy, University College London, Gower Street, London WC1E 6BT, UK
[6] Centre for Astrophysics Research, Science & Technology Research Institute, University of Hertfordshire, Hatfield AL10 9AB, UK
[7] Department of Astronomy, Yonsei University, Seoul 120-749, Korea
[8] Laboratoire AIM, CEA/DSM-CNRS-Université Paris Diderot, DAPNIA/SAp, Orme des Merisiers, 91191 Gif-sur-Yvette, France
[9] Department of Astronomy, California Institute of Technology, Pasadena, CA 91125, USA

ABSTRACT

Residual star formation at late times in early-type galaxies and their progenitors must be suppressed in order to explain the population of red, passively evolving systems we see today. Likewise, residual or newly accreted reservoirs of molecular gas that are fueling star formation must be destroyed. This suppression of star formation in early-type galaxies is now commonly attributed to active galactic nucleus (AGN) feedback wherein the reservoir of gas is heated and expelled during a phase of accretion onto the central supermassive black hole. However, direct observational evidence for a link between the destruction of this molecular gas and an AGN phase has been missing so far. We present new mm-wavelength observations from the IRAM 30 m telescope of a sample of low-redshift SDSS early-type galaxies currently undergoing this process of quenching of late-time star formation. Our observations show that the disappearance of the molecular gas coincides within less than 100 Myr with the onset of accretion onto the black hole and is too rapid to be due to star formation alone. Since our sample galaxies are not associated to powerful quasar activity or radio jets, we conclude that low-luminosity AGN episodes are sufficient to suppress residual star formation in early-type galaxies. This "suppression mode" of AGN feedback is very different from the "truncation mode" linked to powerful quasar activity during early phases of galaxy formation.

Key words: galaxies: active – galaxies: elliptical and lenticular, cD – galaxies: evolution – galaxies: formation

*Online-only material:* color figures

1. INTRODUCTION

The low-redshift galaxy population can be divided into blue star-forming and red passively evolving systems (Baldry et al. 2004). The red population is dominated by elliptical and lenticular (early-type) galaxies, and in order to explain the properties of these systems as we observe them, almost all residual star formation in them must be suppressed. This suppression must take place via the heating or expulsion of the molecular gas which is the fuel for star formation (Dekel & Silk 1986; Benson et al. 2003) and is thought to be driven by the energy input from accreting supermassive black holes at the galaxies' centers in a process called active galactic nucleus (AGN) feedback (Silk & Rees 1998; Benson et al. 2003; Di Matteo et al. 2005; Cattaneo et al. 2005; Kawata & Gibson 2005; Schawinski et al. 2006; Kaviraj et al. 2007a; Khalatyan et al. 2008).

The stellar populations of early-type galaxies indicate that the most massive galaxies are the first to undergo this process of suppression, forming their stars earliest and on the shortest timescales (Thomas et al. 2005; Nelan et al. 2005; Bernardi et al. 2006; Jimenez et al. 2007; Kaviraj et al. 2008a, 2008b). These intense episodes of star formation are followed by passive evolution with almost no subsequent star formation, although evolution via processes such as dry mergers is still possible (e.g., Khochfar & Burkert 2003; van Dokkum 2005). It has been suggested that the mass at which galaxies undergo the transition from star-forming to quiescent decreases over cosmic time (Bell et al. 2005; Bundy et al. 2006), and so less massive galaxies have more extended histories of star formation (Thomas et al. 2005).

As new molecular gas is continuously supplied by accretion, mergers, and stellar mass loss, most current models of galaxy formation suppress residual star formation by invoking a phase of accretion onto the supermassive black hole at the center of the galaxy (Silk & Rees 1998; Cattaneo et al. 2005; Schawinski et al. 2006; Croton et al. 2006) as the energy liberated by core-collapse supernovae is insufficient (Dekel & Silk 1986; Benson et al. 2003). The resulting active galactic nucleus (AGN) phase includes jets, radiation and outflows liberating sufficient energy to destroy the molecular gas reservoir by heating and expelling it, thus suppressing star formation by depriving the host galaxy of its fuel. Observations indicate that the mass of galaxies and their supermassive black holes are correlated (Ferrarese & Merritt 2000; Gebhardt et al. 2000), suggesting that the two co-evolve. The destruction of the gas reservoir may then in turn terminate the growth of the black hole as it deprives itself of material for further accretion as these systems transition to a maintenance mode suppressing cooling flows due to stellar mass loss and cold accretion (Ciotti & Ostriker 1997, 2007; Bower et al. 2006). Alternative, or perhaps complementary, gas heating mechanisms to AGN feedback have been proposed by Birnboim et al. (2007) and Khochfar & Ostriker (2008). Investigating the
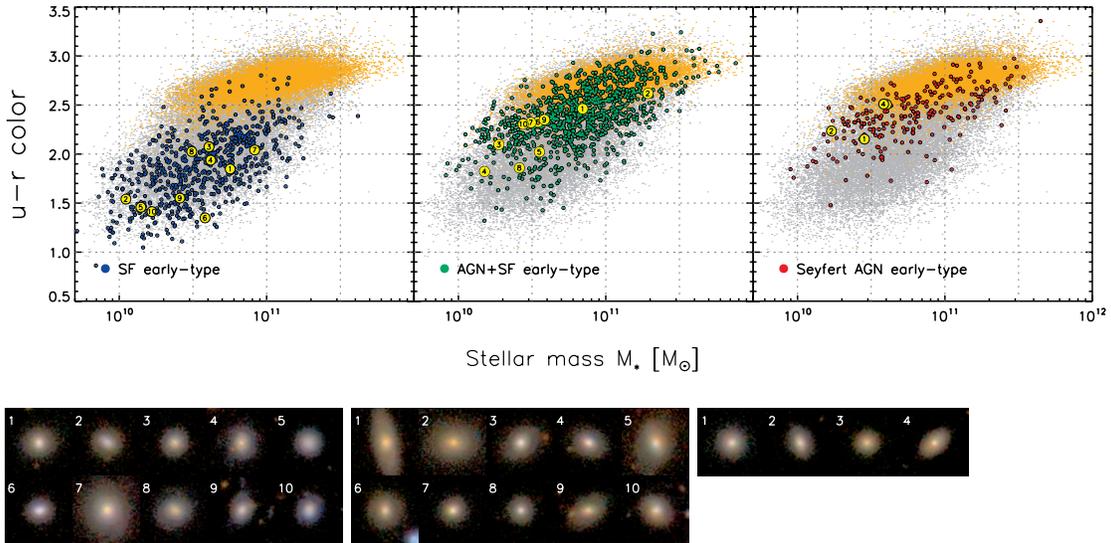
Figure 1. Color–mass relationship for the galaxies in our sample. We plot the galaxy stellar mass derived by spectral energy distribution fitting using the models of Maraston (2005), vs. the optical $u-r$ color. In each panel, morphological late-types are gray, quiescent early-types are orange and the various active early-types (classified by optical emission line ratios) are colored in each panel. From left to right: blue (SF), green (AGN + SF), red (Seyfert AGN). We mark the galaxies observed with the IRAM 30 m telescope with larger points, number them and show their SDSS gri composite color images (Lupton et al. 2004) below in three blocks corresponding to the three classifications. This figure illustrates the progression of early-type galaxies from the blue cloud of star-forming galaxies via an AGN phase to the red sequence of passive galaxies.

(A color version of this figure is available in the online journal.)

role of AGN feedback directly is thus an important observational goal.

Early-type galaxies are known to pass through episodes of accretion onto their central black hole, but evidence which links this phase of their evolution to the removal of the molecular gas reservoir has until now been lacking. In this paper, we present observational evidence for this process occurring in low- to intermediate-mass early-type galaxies at low redshift and identify low-luminosity AGNs as the culprit.

Throughout this work, we assume cosmological parameters ($\Omega_m = 0.3$, $\Omega_\Lambda = 0.7$, $H_0 = 70$), consistent with the *Wilkinson Microwave Anisotropy Probe* (*WMAP*) Third Year results and their combination of results with other data (Spergel et al. 2007).

2. OBSERVING AGN FEEDBACK IN ACTION

We aim to directly observe the effect of AGN on a galaxy's molecular gas as it changes from a star-forming system to a passive early-type galaxy. Schawinski et al. (2007b), hereafter S07, have assembled a sample of approximately 16,000 early-type galaxies from the Sloan Digital Sky Survey (SDSS; York et al. 2000) selected by visual inspection in the redshift range of $0.05 < z < 0.10$. Visual inspection of SDSS images is a powerful method (Fukugita et al. 2004, 2007; Lintott et al. 2008), and ensures the inclusion of early-type galaxies that are still experiencing star formation or host AGNs (Yi et al. 2005; Schawinski et al. 2007a; Kaviraj et al. 2007b). We identify the dominant sources of ionizing radiation as star formation (SF), AGN, or both in each galaxy using ratios of nebular emission lines (Baldwin et al. 1981; Miller et al. 2003; Kewley et al. 2006). We fit the stellar populations using models (Thomas et al. 2003; Maraston 2005), and quantify the age and the mass-fraction of the last significant episode of star formation by combining broadband photometry, from the UV to the near-infrared, with stellar absorption indices measured from optical SDSS spectra.

The star formation history parameters used here are taken from S07, who use a two-burst model for the star formation history. The "old" burst is modeled as a variable single stellar

population (SSP) and the young burst as an exponentially declining burst with an e-folding time of 100 Myr. Tests show that even large shifts in the e-folding time do not generally change the best-fit young age and mass-fraction; only significantly shorter ($\sim$ 10 Myr) or longer ($\sim$ 1 Gyr) e-folding time shift the results and these produce worse fits to the data. The error bars in the young burst age t_y include both formal errors from the fit to the photometry and spectral indices and errors introduced by the choice of parameterization by marginalizing over the other parameters, including dust and metallicity. The marginalization over the variable "old" age accounts for any variation of the star formation *prior* to the most recent event, which is accounted for by the young burst.

S07 find that a large fraction of low- and intermediate-mass early-type galaxies ($50 < \sigma < 150$ km s^{-1}; $10^{10} < M_{\text{stellar}} < 10^{11}$ $M_\odot$) show a clear time sequence (S07; see also Figure 1), which begins with actively star-forming early-type galaxies, which formed typically a few percent of their stellar mass in the most recent episode of star formation. This is followed approximately 200 Myr later by a phase in which both AGN and star formation (AGN + SF) exist together. After the AGN + SF phase, the luminosity of the AGN increases, while all traces of star formation disappear. The Seyfert AGN (SY) phase begins approximately 500 Myr after the beginning of the last episode of star formation. The AGN then declines in luminosity before the galaxy eventually settles into passive evolution in terms of its star formation history, though further evolution via dry mergers may still occur. This striking coincidence between the aging of stellar populations and the rapid evolution of the nebular emission from being excited by star formation to being powered by black hole accretion suggests a role for the AGN in suppressing star formation. A possible caveat on the nature of the SF phase is the possibility that an AGN is present even in the first star-forming phase, but is sufficiently obscured to leave the global ISM unaffected and thus does not influence the optical emission lines. Whether such an obscured AGN already suppresses (or perhaps even drives) star formation is

unclear and further observations are necessary to investigate this question.

Similar observational results have also been presented by Salim et al. (2007), who discuss a possible evolutionary sequence from star formation to quiescence via an AGN phase. The key difference between Salim et al. (2007) and S07 is that S07 consider specifically the early-type galaxy population, and that S07 demonstrate that the galaxies along the sequence from star formation to quiescence via the AGN phase form a genuine evolutionary sequence. Furthermore, Graves et al. (2007) find that at a fixed velocity dispersion, early-type galaxies hosting LINERs are systematically younger than their quiescent counterparts, sampling the penultimate evolutionary phase of S07. The results of S07 favor an AGN feedback interpretation, but cannot rule out alternative explanations.

If the AGNs are responsible for the destruction of the molecular gas, this material should disappear abruptly with the appearance of the AGN in the AGN + SF and Seyfert phase. If, instead, the star formation in these blue early-type galaxies suffices to exhaust or heat the gas reservoir, we should see a steady decline of the amount of molecular gas with time.

In order to test these competing hypotheses, we measure the molecular gas content of a sample of galaxies along this time sequence. Molecular hydrogen is exceedingly difficult to observe directly, so CO, which is an excellent tracer of molecular gas mass (Solomon et al. 1992; Neininger et al. 1998), is commonly used instead.

3. OBSERVATIONS

From S07, we select early-type galaxies with stellar masses from 10^{10} $M_{\odot}$ to 10^{11} $M_{\odot}$, and randomly choose 10 SF, 10 AGN + SF, and four Seyfert AGNs with velocity dispersion $\sigma < 120$ km s^{-1}. The velocity dispersion limit ensures that we select only targets from S07 that are of the type that take part in our AGN feedback time sequence. Objects with higher velocity dispersions typically have older stellar populations, and must have successfully suppressed cooling over long (Gyr) timescales via mechanisms such as LINERs, which are common in such populations. This sample of early-type galaxies spans the transformation from star formation via an AGN phase to quiescence, and so provides us with the ideal laboratory to move from inferring to directly probing the role of AGNs. The difference between selecting galaxies from within categories in this way and randomly selecting galaxies from the entire sample is at a level, which is much less than 2σ (assuming a binomial distribution), and therefore does not produce a significant change in our results.

We observed the CO($1 \rightarrow 0$) transition line in this sample of galaxies along the time sequence with the Institutio de Radioastronomía Milimétrica (IRAM) 30 m telescope at Pico Veleta in 2007 July and December. The IRAM 30 m telescope allowed us to simultaneously also observe the CO($2 \rightarrow 1$) transition. We illustrate our sample selection on the color–mass diagram in Figure 1 and also provide SDSS images of our targets. The spectra were reduced with standard CLASS software and first order polynomial baselines are removed. In Figure 2, we show the reduced spectra, including the fits to line profiles when the CO($1 \rightarrow 0$) transition line is detected. We note that the gas masses derived from our observations are total gas masses. The size of the IRAM beam at the frequency of CO($1 \rightarrow 0$) is $\sim 17\rlap{.}''0$, while the effective radii of our galaxies is on the order of a few arcseconds. We compute the CO luminosity of each target and convert it to a molecular gas mass using a conversion

constant of $\alpha = 1.5$ K km s^{-1}pc^2 (Evans et al. 2005). The derived gas masses and further galaxy properties are in Table 1. The properties of the detected lines are listed in Table 2.

4. RESULTS

The typical molecular gas masses of those nearby early-type galaxies with detections have been estimated to range between 10^6 $M_{\odot}$ and 10^7 $M_{\odot}$ (Sage et al. 2007; Combes et al. 2007), corresponding to very low mass fractions. These previous studies focused on "typical" early-type galaxies drawn from the red sequence population (see also, e.g., Faber & Gallagher 1976; Lake & Schommer 1984). While the gas content of *spiral* AGN hosts has been studied in detail (e.g., Blitz et al. 1986; García-Burillo et al. 2003), no such studies exist for early-type galaxies. Our work is the first to systematically observe gas in early-types systems by mapping the transition from blue to red via an AGN phase and so to investigate the origin of the low gas masses in red early-type galaxies. In light of this, we now consider the results of our observations in both the stacked and individual analysis. We show the results of our observations in Figure 4. In each case, we plot the mass of molecular gas as a function of the time elapsed since the start of the last significant episode of star formation t_y from S07.

In the case of nondetections, we must make an assumption on the expected line profile to determine the amount of gas that would lead to a detection. We divide our analysis into two separate avenues here: first, we perform a very conservative analysis using stacked spectra to establish that we see a trend between age/emission line class and gas fraction. After establishing that a trend exists, we then consider individual galaxies using less conservative upper limits.

4.1. Analysis of Stacked Spectra

We wish to establish the most conservative possible upper limits on our nondetections. Despite the low rms noise levels of our spectra, it is conceivable that a very broad line might lurk just below our sensitivity limits. In order to guard ourselves against this, we stack the nondetected spectra in each emission line class to increase our signal-to-noise and assume the broadest line that can reasonably be expected, a line with FWHM of 300 km s^{-1}. From this, we obtain 2σ gas mass upper limits for the nondetected sources in each class of 10.0, 3.4, and 1.7×10^8 $M_{\odot}$ for the SF, AGN + SF, and Seyfert classes. The stacked spectra for the SF, AGN + SF, and Seyferts are shown in Figure 3; they show no evidence for any lines. For the objects with detected lines, we simply take the mean of the derived gas masses, as stacking might distort the line profile and thus the derived masses.

In panel (a) of Figure 4, we show the mean gas masses of those galaxies which are detected in both the SF and the AGN + SF classes. We furthermore show the upper limits for the stacked nondetections assuming a very conservative line width of 300 km s^{-1}. The star-forming early-type galaxies at young ages have high molecular gas masses of the order of up to $\sim 10^9$ $M_{\odot}$. On the other hand, the pure (Seyfert) AGN where no traces of ongoing star formation are left in the optical emission lines are undetected in CO with upper limits on the gas mass significantly lower than the younger SF objects. In between lie the AGN + SF objects: the detections are systematically younger and have mean gas masses slightly below the SF objects. The nondetected AGN + SF objects are older than their detected counterparts, but younger than the
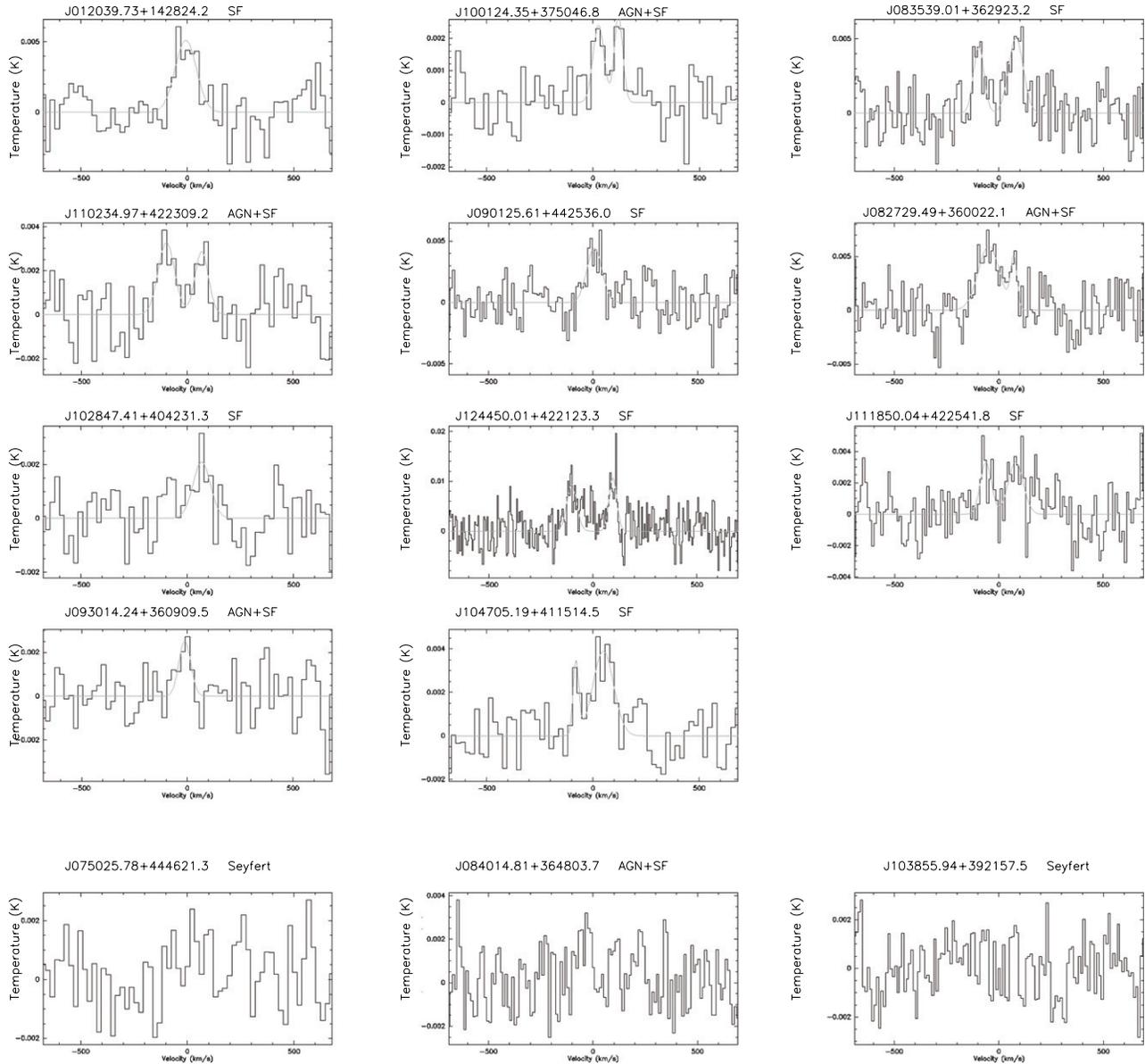
Figure 2. CO(1 → 0) line profiles for our targets. We plot the temperature as a function of velocity measured from the redshift of the host galaxy. For each object, we give the SDSS name and emission line classification (SF, AGN + SF, Seyfert). In the top four rows, we show the detections, while in the bottom row, we show a sample of three non-detections. For the detections, we indicate the best-fit line profile from our CLASS data reduction. Note that all detected lines are relatively narrow (∼ 70 km s^{-1}) and many objects show double-peaked profiles.

Seyferts. During in the AGN + SF phase, at about 200 Myr after the onset of star formation, the molecular gas mass drops precipitously.

It should be noted that the presence of CO correlates with other measures of star formation and so galaxies with more CO have more vigorous star formation (Kennicutt 1998; Gao & Solomon 2004; Narayanan et al. 2005). However, the star formation history parameters derived by S07 would account for the implied larger mass fraction in the young population and still return the correct age for it.

4.2. Analysis of Individual Spectra

On the basis that we can establish the significance of the observed trend in panel (a) of Figure 4 using the stacked spectra, we now turn to individual galaxies. Since S07 resolve the age of the current episode of star formation and provide emission line classes for each individual object, we can also plot these to reveal trends within populations. Half of our detections shows single, narrow CO(1 → 0) lines. The other half shows two components. The median FWHM of the single lines and the individual components is 70 km s^{-1}. These relatively moderate widths are consistent with the fact that the galaxies in our sample are only intermediate-mass objects and that they are undergoing minor residual star formation. They are not undergoing major starbursts requiring enormous gas reservoirs, nor are they spiral galaxies with extended disks with broad double-horned lines.

In the absence of comparable samples, we use the median FWHM of our sources with detections of 70 km s^{-1} to estimate the upper limits on the gas mass in the non-detections. These are not as rigorous as the limits of the stacked spectra, but as we will show, the results are consistent. With this analysis, we neglect the possibility of double-horned profiles in the analysis, which would increase the upper limits of the nondetections by up to a factor 2. The analysis of the stacked spectra however does not support this latter scenario.

Table 1
SDSS & IRAM Data

SDSS Object Name	R.A. (J2000)	Decl. (J2000)	Emission Line Class[a]	Stellar Mass $M_{stellar}$ ($\times 10^{10}\,M_\odot$)	Total CO Flux[b] $S_{CO(1\to0)}$ (K km s^{-1})	Molecular Gas Mass[c] M_{gas} ($\times 10^8\,M_\odot$)	Age of Starburst[d] t_y (Myr)
SDSS J075109.77+342636.5	07 51 09.8	+34 26 36.6	SF	5.7 ± 1.03	< 0.07	< 1.88	180^{70}_{-70}
SDSS J012039.73+142824.2	01 20 39.7	+14 28 24.2	SF	1.1 ± 0.07	0.63 ± 0.19	6.0 ± 1.89	70^{40}_{-40}
SDSS J002227.39+135430.6	00 22 27.4	+13 54 30.6	SF	4.1 ± 0.31	< 0.07	< 2.03	340^{70}_{-60}
SDSS J011458.35+142726.3	01 14 58.4	+14 27 26.4	AGN + SF	7.0 ± 1.12	< 0.14	< 2.90	540^{80}_{-80}
SDSS J000336.67+141433.9	00 03 36.7	+14 14 34.0	AGN + SF	19.3 ± 1.67	< 0.14	< 5.26	1990^{1480}_{-1720}
SDSS J100124.35+375046.8	10 01 24.4	+37 50 46.9	AGN + SF	1.9 ± 0.28	0.28 ± 0.055	2.5 ± 0.49	460^{200}_{-200}
SDSS J083539.01+362923.2	08 35 39.0	+36 29 23.2	SF	4.2 ± 0.43	0.73 ± 0.10	7.5 ± 1.04	200^{70}_{-70}
SDSS J110234.97+422309.2	11 02 35.0	+42 23 09.2	AGN + SF	1.5 ± 0.27	0.56 ± 0.11	6.5 ± 1.35	150^{80}_{-60}
SDSS J090125.61+442536.0	09 01 25.6	+44 25 36.0	SF	1.4 ± 0.25	0.39 ± 0.070	3.8 ± 0.68	190^{40}_{-40}
SDSS J082729.49+360022.1	08 27 29.5	+36 00 22.1	AGN + SF	3.5 ± 0.59	0.97 ± 0.16	9.6 ± 1.66	150^{100}_{-90}
SDSS J082104.65+412108.5	08 21 04.7	+41 21 08.6	AGN + SF	3.5 ± 0.63	< 0.07	< 1.65	310^{190}_{-130}
SDSS J102847.41+404231.3	10 28 47.4	+40 42 31.4	SF	3.8 ± 1.11	0.53 ± 0.1	5.3 ± 1.00	190^{40}_{-40}
SDSS J124450.01+422123.3	12 44 50.0	+42 21 23.4	SF	8.3 ± 1.69	1.38 ± 0.190	13.4 ± 1.84	140^{100}_{-90}
SDSS J125716.71+424625.9	12 57 16.7	+42 46 26.0	SF	3.1 ± 0.19	< 0.21	< 4.09	310^{120}_{-110}
SDSS J075025.78+444621.3	07 50 25.8	+44 46 21.3	Seyfert	2.8 ± 0.31	< 0.07	< 1.18	470^{150}_{-140}
SDSS J111850.04+422541.8	11 18 50.0	+42 25 41.8	SF	2.6 ± 0.47	0.55 ± 0.10	6.2 ± 1.13	170^{50}_{-50}
SDSS J084014.81+364803.7	08 40 14.8	+36 48 03.7	AGN + SF	3.1 ± 0.58	< 0.07	< 1.45	900^{460}_{-500}
SDSS J103855.94+392157.5	10 38 55.9	+39 21 57.6	Seyfert	1.7 ± 0.24	< 0.07	< 1.40	960^{330}_{-380}
SDSS J093014.24+360909.5	09 30 14.2	+36 09 09.6	AGN + SF	2.6 ± 0.53	0.17 ± 0.065	2.1 ± 0.79	100^{70}_{-80}
SDSS J082115.75+355924.6	08 21 15.8	+35 59 24.7	Seyfert	4.0 ± 0.41	< 0.07	< 1.68	1080^{660}_{-430}
SDSS J082507.10+410319.4	08 25 07.1	+41 03 19.5	AGN + SF	3.8 ± 0.60	< 0.07	< 1.51	220^{170}_{-120}
SDSS J084216.23+360141.4	08 42 16.2	+36 01 41.5	Seyfert	3.8 ± 0.35	< 0.07	< 1.37	1740^{1020}_{-1150}
SDSS J104705.19+411514.5	10 47 05.2	+41 15 14.5	SF	1.7 ± 0.31	0.34 ± 0.090	3.4 ± 0.89	190^{40}_{-40}
SDSS J103843.56+404221.0	10 38 43.6	+40 42 21.0	AGN + SF	2.8 ± 0.49	< 0.07	< 1.39	890^{380}_{-440}

Notes.

[a] BPT emission line classification, described in detail in Schawinski et al. (2007a).

[b] Upper limits for the total CO flux are based on the rms noise of the smoothed spectrum and assuming a line of width 70 km s^{-1}, they are 1σ limits.

[c] Molecular gas masses are derived from the total CO luminosity and assuming a conversion from CO to molecular gas mass of $\alpha = 1.5$ K km s^{-1}pc^2 (Evans et al. 2005). The gas mass upper limits are 2σ as in the Figures.

[d] The age of the last episode of star formation t_y is taken from Schawinski et al. (2007a) and is based on fitting the UV/optical/NIR spectral energy distribution and the stellar (Lick) absorption indices.

The individual galaxies show the same trend and allow us some insight into variations within each population. We present these in panel (b) of Figure 4 and the gas masses and ages t_y are given in Table 1. We see here that the SF molecular gas masses are within a factor of a few of each other and reach up to $\sim 10^9\,M_\odot$. All three Seyfert AGNs are individually undetected. In between are the AGN + SF objects, two of which have high masses with the remainder either undetected or significantly lower than the star-forming galaxies. Figure 4(b) shows the same trend as Figure 4(a). The individual gas masses and upper limits further support the observation that the gas mass drops precipitously at ~ 200 Myr within the AGN + SF phase.

To assess the significance of the difference between the populations we divide the sample into two groups, one younger than 200 Myr and one older. We use Bayes' theorem to find the posterior distribution of the population mean and variance of the two groups' molecular gas masses by assuming that each group is drawn from a different normal distribution. Samples on which only upper limits were found are described as Gaussian data points with zero mean and the appropriate width. We place a flat prior on the population means and standard deviations. After computing the joint posteriors, we marginalize over the standard deviation. The result is a probability distribution for each of the two populations means regardless of their variances. Together the distributions show that the younger group has a higher mean with $> 95\%$ probability.

Table 2
IRAM Data Line Properties[a]

SDSS Object Name[b]	Line Width km s^{-1}	Line Peak K
SDSS J012039.73+142824.2	120 ± 20	5.1×10^{-3}
SDSS J100124.35+375046.8	60 ± 25	2.4×10^{-3}
"	35 ± 12	3.3×10^{-3}
SDSS J083539.01+362923.2	55 ± 18	4.5×10^{-3}
"	80 ± 17	5.1×10^{-3}
SDSS J110234.97+422309.2	87 ± 25	3.2×10^{-3}
"	71 ± 28	2.8×10^{-3}
SDSS J090125.61+442536.0	85 ± 15	4.5×10^{-3}
SDSS J082729.49+360022.1	120 ± 22	5.9×10^{-3}
"	37 ± 25	4.7×10^{-3}
SDSS J102847.41+404231.3	60 ± 28	1.7×10^{-3}
"	96 ± 43	2.2×10^{-3}
SDSS J124450.01+422123.3	120 ± 22	6.4×10^{-3}
"	43 ± 7	1.0×10^{-3}
SDSS J111850.04+422541.8	20 ± 8	4.4×10^{-3}
"	260 ± 60	2.1×10^{-3}
SDSS J093014.24+360909.5	65 ± 30	2.5×10^{-3}
SDSS J104705.19+411514.5	18 ± 10	5.4×10^{-3}
"	116 ± 26	3.9×10^{-3}

Notes.

[a] Only for those with CO($1 \to 0$) detections.

[b] Objects with two components are listed twice with each component line profile parameters separately.
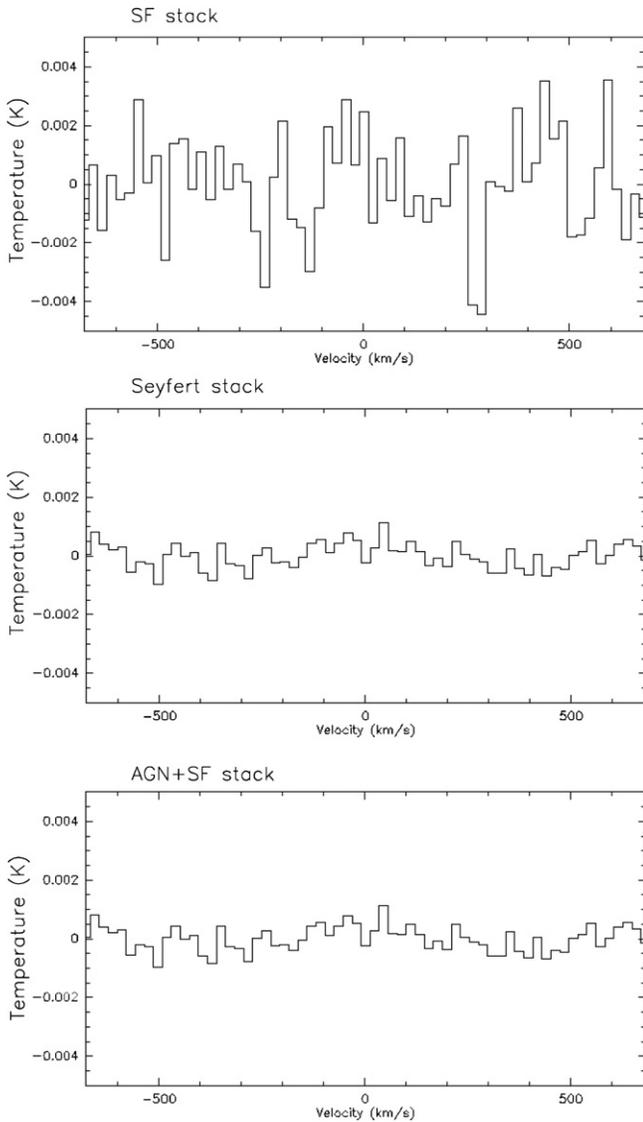
Figure 3. CO(1 → 0) stacked spectra for the Seyferts and the AGN + SF non-detections. Assuming a very broad line as a worst-case scenario with a FWHM of 300 km s^{-1}, the 2σ gas mass upper limit of the SF, SF + AGN and Seyfert stacks are 10.0, 3.4 and $1.7 \times 10^8\ M_\odot$.

4.3. The Case for AGN Feedback: the Schmidt Law and Gas Depletion Timescales

Such a sudden drop in molecular gas mass as we observe cannot be accounted for by star formation alone. To demonstrate this, we compute the evolution of the molecular gas mass for both the mean SF galaxy and each of the SF early-types with CO(1 → 0) detections, using the Schmidt law for star formation (Schmidt 1959; Kennicutt 1998):

$$\mathrm{SFR} = \frac{\epsilon M_{\mathrm{gas}}}{t_{\mathrm{dyn}}}. \qquad (1)$$

We assume a fiducial efficiency of 2% ($\epsilon = 0.02$), which includes the effect of SN feedback. This law appears to be universally applicable across galaxy morphologies, including early-type galaxies (Combes et al. 2007). We compute the dynamical times of each galaxy from its radius and stellar mass ($t_{\mathrm{dyn}} = \sqrt{R^3/2GM}$); for the stacked SF galaxies, we use the median t_{dyn} of 50 Myr of the SF galaxies. We show the resulting evolutionary tracks in Figures 4(a) and (c) (dashed lines).

The depletion timescales derived this way from the Schmidt Law are on the order of several Gyrs, much longer than the observed timescale for gas depletion. The tracks shown in Figures 4(a) and (c) are inconsistent with a scenario where star formation alone depletes the gas reservoir.

Would it be possible to adjust the parameters used to result in tracks for star formation alone that are consistent with our observations? Adjusting the mass and radius to achieve the rapid gas reservoir exhaustion we observe results in parameters not characteristic of a galaxy-wide starburst, but perhaps a circumnuclear ring. Alternatively, a drastic increase of the star formation efficiency ϵ toward unity driven by an AGN (Silk 2005) might suffice, though this completes the circle and brings us back to AGN feedback. Our modeling does *not* account for the amount of recycled gas from stellar mass loss or further gas accreted, both of which would further increase the amount of molecular gas available over time and thus extend the depletion timescales significantly. This caveat further strengthens our argument against star formation alone.

This decrease in molecular gas coincides with the time when galaxies transition from pure star formation to an AGN + SF composite as the AGN switches on of ∼ 200 Myr (S07). Figure 5 shows this same trend in the emission line diagnostic diagrams. There the two AGN + SF composites with the gas masses similar to the star-forming objects reside in close proximity to them; those AGN + SF objects further away from the star-forming locus are either undetected or have significantly lower gas masses.

5. DISCUSSION

Models of hierarchical galaxy formation suggest that AGN feedback plays an important role in the formation and late-time evolution of early-type galaxies. Current simulations invoke two modes of black hole growth and AGN feedback: a "quasar mode" (e.g., Springel et al. 2005; Di Matteo et al. 2005; Hopkins et al. 2008) and a "radio mode" (e.g., Croton et al. 2006; Bower et al. 2006; Sijacki et al. 2007).

5.1. Two Modes of AGN Feedback

The quasar mode, implemented in simulations such as that of Springel et al. (2005), assumes that during a major merger a fraction of the rest mass of the gas accreted onto the central black hole is liberated as energy injected back isotropically into the gas reservoir of the host galaxy. Simulations of gas-rich mergers at very high redshift (Narayanan et al. 2006; Li et al. 2007; Narayanan et al. 2008) indicate that quasars might be driving massive, powerful outflows as the energy liberated by black hole accretion is coupled to the gas in the form of thermal energy. These outflows may succeed in halting star formation on short timescales (Hamann & Ferland 1992), as required for the most massive early-type galaxies (Thomas et al. 2005). On the other hand, observations of quasars at high redshift yield very high CO luminosities and hence high inferred gas masses (Cox et al. 2002; Bertoldi et al. 2003; Walter et al. 2004), which suggests that feedback in these objects does not necessarily result in the instantaneous removal of molecular gas from the system.

The radio mode (Croton et al. 2006; Bower et al. 2006; Khalatyan et al. 2008), instead, is important for the evolution of galaxies and is supposed to occur at later times. A low-level AGN is thought to be injecting a fraction of the rest mass energy of the hot gas accreted by the central black hole into the ISM over an extended period of time to keep the host galaxy quiescent.
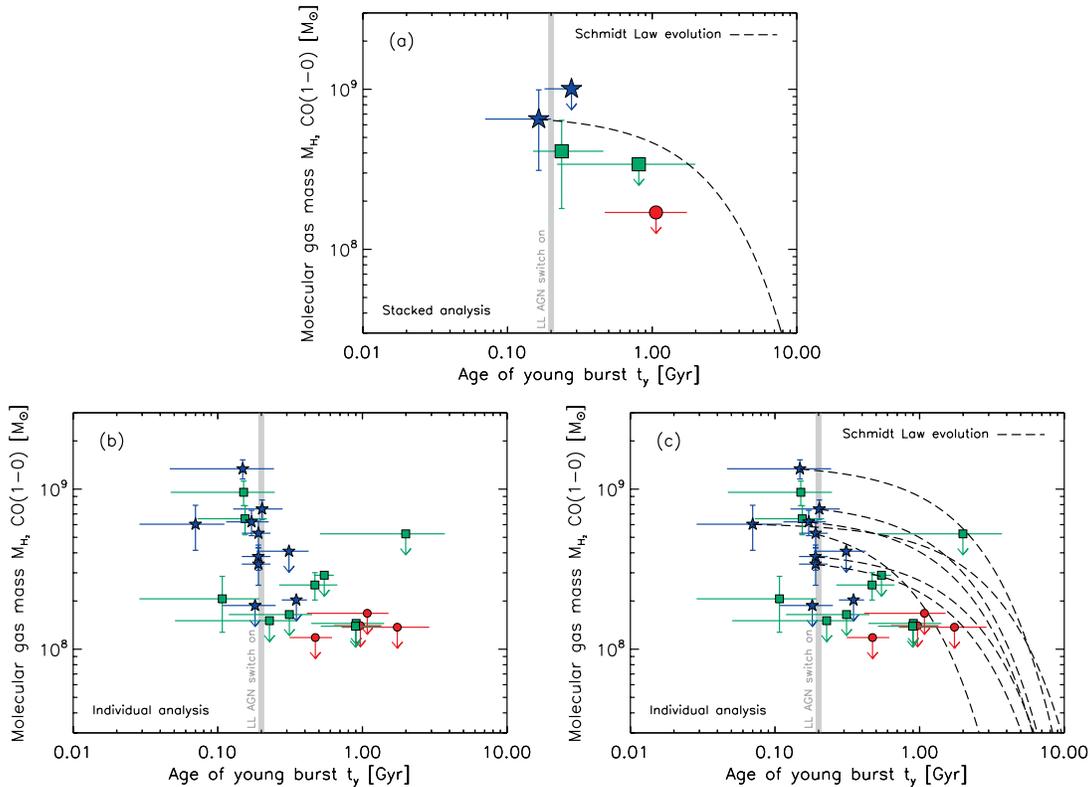
Figure 4. Observed molecular gas masses M_{H_2} as a function of t_y, the age of the last significant episode of star formation (Schawinski et al. 2007b). The blue stars are early-type galaxies classified as star-forming, the green squares are AGN + SF composites and the red circles are Seyfert AGN. In the top panel, we show the results from the analysis of the stacked spectra. The upper limits are 2σ assuming a typical linewidth of 300 km s^{-1}. In the bottom panels, (b) and (c), we show the individual gas masses for each galaxy. The upper limits are 2σ assuming a typical linewidth of 70 km s^{-1}. The values of t_y are based on assuming an e-folding time of 100 Myr for the starburst; allowing this time to vary simply extends the error bars, but does not move the best-fit values. Instantaneous bursts or constant star formation models yield poor fits to the data. In panels (a) and (c), we show the tracks showing the future evolution of the gas mass assuming the Schmidt Law for star formation. In (a), we show this track for the mean SF galaxy, whereas in (c), we show tracks for each individually detected SF galaxy. These tracks illustrate that given an evolution driven purely by star formation, the depletion of the gas reservoirs on the short timescales we observe is not feasible. These tracks assumes a dynamical timescale of $\tau = 100$ Myr and are inconsistent with the systematically lower gas masses of the AGN + SF objects, whether detected or not. We mark the point in time $t_y = 200$ Myr when the low-luminosity AGNs in the AGN + SF objects typical switch on.

(A color version of this figure is available in the online journal.)
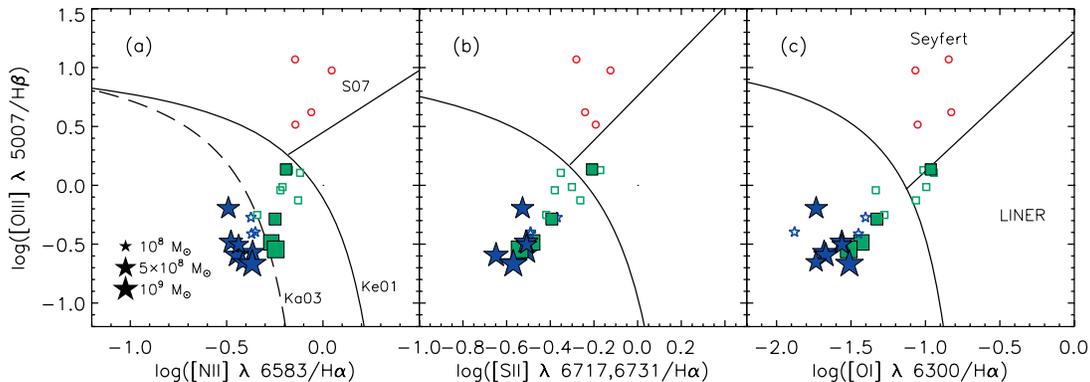
Figure 5. Objects in our sample on emission line diagrams (Baldwin et al. 1981; Kewley et al. 2001; Kauffmann et al. 2003; Kewley et al. 2006). In panel (a), we delineate star-forming galaxies by the dashed line (Ka03; Kauffmann et al. 2003). Between the dashed and solid line (Ke01) reside AGN + SF composites, while beyond the solid line there are the pure AGN (Kewley et al. 2001). The straight line (S07) divides Seyfert AGN from LINERs. The blue stars represent star-forming early-type galaxies, the green squares AGN + SF composites and the red circles Seyfert AGN. Filled symbols are CO(1 → 0) detections and open symbols are nondetections. The size of the symbol scales with the logarithm of the molecular gas mass (see legend in (a)). In panels (b) and (c), we show a similar line ratio diagram using the classification of Kewley et al. (2006). The species [S II] and [O I] used in (b) and (c) are sensitive to low ionization states and complement (a) based on [N II]. Note that the two AGN + SF galaxies with large molecular gas masses are also modest radio sources.

(A color version of this figure is available in the online journal.)

5.2. Molecular Gas Reservoir Destruction by Low-Luminosity AGNs

Our galaxies help us illuminate the role of AGNs in suppressing late-time star formation. In previous work (S07) we

have identified a sample of low- and intermediate-mass early-type galaxies that display an evolutionary sequence from minor star formation through AGN to the red sequence, most likely driven by AGN feedback. In the present paper we investigate through IRAM mm-observations the presence and absence of

cold, molecular gas reservoirs in objects selected along this sequence.

The results presented here support the presence of late-time AGN feedback invoked in the simulations. Our observations suggest a scenario in which molecular gas is removed or heated $\sim$ 200 Myr after the peak of recent star formation in our systems. Most importantly, this observed drop coincides with the timescale on which these galaxies transition from being primarily star forming to being dominated by AGN. We show that significantly longer timescales would be expected if the molecular gas was to be consumed by star formation alone.

The AGN detected in our sample are low-luminosity AGNs. They are neither powerful quasars nor radio-loud. Their accretion rates and efficiencies are low ($10^6 < L_{[O III]} < 10^8 L_\odot$, $-3 < \log(L_{[O III]}/\sigma^4) < 0$; S07).[10] Out of our entire sample only two targets are detected at 1.4 GHz by the VLA FIRST Survey (Becker et al. 1995) at a detection limit of 3×10^{21} W Hz^{-1}, both of which are AGN + SF objects with modest $L_{1.4 \text{ GHz}}$ of 6.7×10^{21} W Hz^{-1} and 2.5×10^{22} W Hz^{-1}. These two AGN + SF objects are those with the two highest molecular gas masses.

Some theoretical models have discussed scenarios where low-luminosity, low-accretion-efficiency AGNs of the kind we see here regulate star formation (Hopkins & Hernquist 2006; Ciotti & Ostriker 2007). Furthermore, the time delay between peak SF and AGN Eddington ratio and the moment of "blowout"—when the AGN drives out the gas reservoir—is present in the models of Hopkins & Hernquist (2006) and Hopkins et al. (2006). The process we see thus might be physically similar to quasar mode feedback as envisioned by theorists, but fulfills the task of the radio mode in moderate-mass early-type galaxies of suppressing further late-time star formation.

We conclude that low-level AGNs appear to be powerful enough to destroy the molecular gas reservoir and suppress star formation in early-type galaxies. Furthermore, we note that along the time sequence established and described by S07, the peak of the AGN accretion rate and efficiency occur during the Seyfert phase; the AGN phase that suppresses star formation is less efficient than this peak.

5.3. Suppression vs. Truncation

At high redshift, early-type galaxies (or their progenitors) experience vigorous star formation. The large energy output from quasar-like AGNs is required to bring such massive star formation to a halt. We refer to this type of AGN feedback as "truncation mode". In order to account for the observed high star formation efficiency in these galaxies, it is possible that a "trigger mode" may precede the truncation mode (Silk 2005).

Clearly, the process we are probing with the present work is very different. We see AGN feedback operating at late times in early-type galaxies associated with low-luminosity AGN. No quasar-like activity or powerful radio jets are observed. We witness the suppression of star formation in early-type galaxies at recent epochs. We, therefore, prefer to call this type of AGN feedback "suppression mode" as opposed to the truncation mode at early times. The low- and intermediate-mass galaxies studied in our undergo very minor episodes of star formation and thus allow us to study this suppression process. Apparently, the AGN

---

[10] The quantity $L_{[O III]}/\sigma^4$, introduced by Kewley et al. (2006), is a proxy of the Eddington ratio. $L_{[O III]}$ traces the accretion rate, while σ^4 traces the black hole mass via the $M_\bullet$–σ relation (Gebhardt et al. 2000; Ferrarese & Merritt 2000).

in this lower mass range is not powerful enough to inhibit residual star formation completely (see also Schawinski et al. 2006). As shown in Figure 4, however, without the energy input from AGNs, those episodes of star formation would be more significant and would drive the objects even further away from the red sequence. The observed suppression by AGN feedback ensures that these objects will join or return to passive evolution on the red sequence. Note that the massive early-type galaxies in our sample, instead, do not show any signs of residual star formation. As discussed in S07, the LINER activity detected in some of them might be the "smoking gun" of highly effective suppression mode AGN feedback.

Finally, it is interesting to note that the suppression mode detected here acts on timescales around several hundred Myr, which is the typical timescale of an AGN duty cycle. Hence, suppression of residual star formation in early-type galaxies at late times may not be a continuous but a periodic process (see e.g., Ciotti & Ostriker 2007).

6. CONCLUSIONS

The molecular gas reservoirs fueling late time star formation in early-type galaxies must be destroyed to account for their passive evolution on the red sequence. This suppression of star formation in early-type galaxies is now commonly attributed to AGN feedback wherein the reservoir of gas is heated and expelled by the energy input from an accretion phase onto the central supermassive black hole. In this paper, we present observational evidence for this process occurring in low- to intermediate-mass early-type galaxies at low redshift and identify low-luminosity AGNs—not quasars or radio galaxies—as the culprit. The systems studied here are not the massive galaxies in clusters where the radio mode is generally invoked to suppress cooling.

In order to empirically determine whether and at which stage AGNs are involved in the destruction of significant molecular gas reservoirs, we perform an observational investigation. We have observed a sample of low-redshift intermediate mass early-type galaxies during the process of moving from the blue cloud to the red sequence via a low-luminosity AGN phase. We observed galaxies along the time sequence of S07 with the IRAM 30m telescope near Granada, Spain to determine the amounts of molecular gas present via the CO(1 $\rightarrow$ 0) line.

We perform two separate analyses: first, we take the average gas masses in each of the SF, SF + AGN, and Seyferts galaxies, and stack the spectra of the non-detections to increase signal-to-noise and, therefore, the upper limit on the gas mass. For the non-detections, we assume an extremely conservative line width of 300 km s^{-1}, and find a statistically significant trend. The gas mass in the SF galaxies drops approximately 200 Myr after the start of star formation, during the AGN + SF phase, and is far too rapid to be accounted for by star formation alone. None of the four Seyfert AGNs were detected, suggesting that the gas reservoirs were already destroyed in the preceding AGN + SF phase, i.e., prior to the peak AGN luminosity and accretion efficiency (see S07). The molecular gas reservoir drops by at least an order of magnitude in mass in a very short time. The Schmidt law for star formation implies depletion timescales of several Gyr, even if contributions such as further accretion, cooling and mass-loss by evolved stars is ignored. We thus interpret the low-luminosity AGN in the AGN + SF phase as the culprit responsible for the destruction of the gas reservoir. It is possible that the feedback work of the AGN might have begun in an obscured fashion during the SF phase,

during which the feedback from stars might have aided the gas removal.

Second, we perform the same analysis for each galaxy assuming a measured line width of 70 km s^{-1} for the non-detected galaxies. We find the same trend: star-forming early-type galaxies have substantial molecular gas reservoirs. A few AGN + SF early-types are detected with diminished gas reservoirs, while others are undetected, with gas masses inferred to be at least an order of magnitude lower. The individual galaxy data points show that the depletion of the molecular gas reservoir occurs within the AGN + SF phase about 200 Myr after the start of star formation. The Seyfert AGN are all undetected. For the individual galaxies, we perform a Bayesian significance test and find significant evidence for populations of galaxies with star formation more recent than 200 Myr and older than this value having different molecular gas masses.

We then discuss the implications of our result and how it impacts our understanding of AGN feedback. The process we see occurring suppresses residual star formation in intermediate-mass, low-redshift galaxies and so could be termed a "suppression mode" of the AGN, which maintains the red colors of early-type galaxies by suppressing residual star formation. This mode stands in contrast to the "truncation mode" which is thought to shut down star formation during the formation of massive galaxies at high redshift.

The AGN phase responsible for this suppression mode is a low-luminosity event and not a powerful quasar or radio galaxy phase. The fact that we observe low-luminosity AGN impacting the fuel for star formation in early-type galaxies is an important step toward understanding galaxy formation.

REFERENCES

Baldry, I. K., Glazebrook, K., Brinkmann, J., Ivezić, Ž., Lupton, R. H., Nichol, R. C., & Szalay, A. S. 2004, ApJ, 600, 681
Baldwin, J. A., Phillips, M. M., & Terlevich, R. 1981, PASP, 93, 5
Becker, R. H., White, R. L., & Helfand, D. J. 1995, ApJ, 450, 559
Bell, E. F., et al. 2005, ApJ, 625, 23
Benson, A. J., Bower, R. G., Frenk, C. S., Lacey, C. G., Baugh, C. M., & Cole, S. 2003, ApJ, 599, 38
Bernardi, M., Nichol, R. C., Sheth, R. K., Miller, C. J., & Brinkmann, J. 2006, AJ, 131, 1288
Bertoldi, F., et al. 2003, A&A, 409, L47
Birnboim, Y., Dekel, A., & Neistein, E. 2007, MNRAS, 380, 339
Blitz, L., Mathieu, R. D., & Bally, J. 1986, ApJ, 311, 142
Bower, R. G., Benson, A. J., Malbon, R., Helly, J. C., Frenk, C. S., Baugh, C. M., Cole, S., & Lacey, C. G. 2006, MNRAS, 370, 645
Bundy, K., et al. 2006, ApJ, 651, 120
Cattaneo, A., Blaizot, J., Devriendt, J., & Guiderdoni, B. 2005, MNRAS, 364, 407

Ciotti, L., & Ostriker, J. P. 1997, ApJ, 487, L105+
Ciotti, L., & Ostriker, J. P. 2007, ApJ, 665, 1038
Combes, F., Young, L. M., & Bureau, M. 2007, MNRAS, 377, 1795
Cox, P., et al. 2002, A&A, 387, 406
Croton, D. J., et al. 2006, MNRAS, 365, 11
Dekel, A., & Silk, J. 1986, ApJ, 303, 39
Di Matteo, T., Springel, V., & Hernquist, L. 2005, Nature, 433, 604
Evans, A. S., Mazzarella, J. M., Surace, J. A., Frayer, D. T., Iwasawa, K., & Sanders, D. B. 2005, ApJS, 159, 197
Faber, S. M., & Gallagher, J. S. 1976, ApJ, 204, 365
Ferrarese, L., & Merritt, D. 2000, ApJ, 539, L9
Fukugita, M., Nakamura, O., Turner, E. L., Helmboldt, J., & Nichol, R. C. 2004, ApJ, 601, L127
Fukugita, M., et al. 2007, AJ, 134, 579
Gao, Y., & Solomon, P. M. 2004, ApJ, 606, 271
García-Burillo, S., et al. 2003, A&A, 407, 485
Gebhardt, K., et al. 2000, ApJ, 539, L13
Graves, G. J., Faber, S. M., Schiavon, R. P., & Yan, R. 2007, ApJ, 671, 243
Hamann, F., & Ferland, G. 1992, ApJ, 391, L53
Hopkins, P. F., Cox, T. J., Kereš, D., & Hernquist, L. 2008, ApJS, 175, 390
Hopkins, P. F., & Hernquist, L. 2006, ApJS, 166, 1
Hopkins, P. F., Hernquist, L., Cox, T. J., Robertson, B., Di Matteo, T., & Springel, V. 2006, ApJ, 639, 700
Jimenez, R., Bernardi, M., Haiman, Z., Panter, B., & Heavens, A. F. 2007, ApJ, 669, 947
Kauffmann, G., et al. 2003, MNRAS, 346, 1055
Kaviraj, S., Kirkby, L. A., Silk, J., & Sarzi, M. 2007a, MNRAS, 382, 960
Kaviraj, S., et al. 2007b, ApJS, 173, 619
Kaviraj, S., et al. 2008a, MNRAS, 388, 67
Kaviraj, S. 2008b, Mod. Phys. Lett. A, 23, 153
Kawata, D., & Gibson, B. K. 2005, MNRAS, 358, L16
Kennicutt, Jr R. C., 1998, ApJ, 498, 541
Kewley, L. J., Dopita, M. A., Sutherland, R. S., Heisler, C. A., & Trevena, J. 2001, ApJ, 556, 121
Kewley, L. J., Groves, B., Kauffmann, G., & Heckman, T. 2006, MNRAS, 372, 961
Khalatyan, A., Cattaneo, A., Schramm, M., Gottlöber, S., Steinmetz, M., & Wisotzki, L. 2008, MNRAS, 387, 13
Khochfar, S., & Burkert, A. 2003, ApJ, 597, L117
Khochfar, S., & Ostriker, J. P. 2008, ApJ, 680, 54
Lake, G., & Schommer, R. A. 1984, ApJ, 280, 107
Li, Y., et al. 2007, ApJ, 665, 187
Lintott, C. J., et al. 2008, MNRAS, 389, 1179
Lupton, R., Blanton, M. R., Fekete, G., Hogg, D. W., O'Mullane, W., Szalay, A., & Wherry, N. 2004, PASP, 116, 133
Maraston, C. 2005, MNRAS, 362, 799
Miller, C. J., Nichol, R. C., Gómez, P. L., Hopkins, A. M., & Bernardi, M. 2003, ApJ, 597, 142
Narayanan, D., Groppi, C. E., Kulesa, C. A., & Walker, C. K. 2005, ApJ, 630, 269
Narayanan, D., et al. 2006, ApJ, 642, L107
Narayanan, D., et al. 2008, ApJS, 174, 13
Neininger, N., Guelin, M., Ungerechts, H., Lucas, R., & Wielebinski, R. 1998, Nature, 395, 871
Nelan, J. E., et al. 2005, ApJ, 632, 137
Sage, L. J., Welch, G. A., & Young, L. M. 2007, ApJ, 657, 232
Salim, S., et al. 2007, ApJS, 173, 267
Schawinski, K., et al. 2006, Nature, 442, 888
Schawinski, K., et al. 2007a, ApJS, 173, 512
Schawinski, K., Thomas, D., Sarzi, M., Maraston, C., Kaviraj, S., Joo, S.-J., Yi, S. K., & Silk, J. 2007b, MNRAS, 382, 1415
Schmidt, M. 1959, ApJ, 129, 243
Sijacki, D., Springel, V., di Matteo, T., & Hernquist, L. 2007, MNRAS, 380, 877
Silk, J. 2005, MNRAS, 364, 1337
Silk, J., & Rees, M. J. 1998, A&A, 331, L1
Solomon, P. M., Downes, D., & Radford, S. J. E. 1992, ApJ, 387, L55
Spergel, D. N., et al. 2007, ApJS, 170, 377
Springel, V., Di Matteo, T., & Hernquist, L. 2005, MNRAS, 361, 776
Thomas, D., Maraston, C., & Bender, R. 2003, MNRAS, 339, 897
Thomas, D., Maraston, C., Bender, R., & Mendes de Oliveira, C. 2005, ApJ, 621, 673
van Dokkum, P. G. 2005, AJ, 130, 2647
Walter, F., et al. 2004, ApJ, 615, L17
Yi, S. K., et al. 2005, ApJ, 619, L111
York, D. G., et al. 2000, AJ, 120, 1579